EXPLOITING CORRELATION IN NEURAL SIGNALS FOR DATA COMPRESSION

S. Schmale*, J. Hoeffmann*, B. Knoop*, G. Kreiselmeyer† , H. Hamer†, D. Peters-Drolshagen*, S. Paul*

*Institute of Electrodynamics and Microelectronics (ITEM.me), University of Bremen, Germany
{schmale, hoeffmann, knoop, peters, steffen.paul}@me.uni-bremen.de
†Epilepsy Center of Erlangen (EZE), University Hospital of Erlangen, Germany
{gernot.kreiselmeyer, hajo.hamer}@uk-erlangen.de

ABSTRACT

Progress in invasive brain research relies on signal acquisition at high temporal- and spatial resolutions, resulting in a data deluge at the (wireless) interface to the external world. Hence, data compression at the implant site is necessary in order to comply with the neurophysiological restrictions, especially when it comes to recording and transmission of neural raw data. This work investigates spatial correlations of neural signals, leading to a significant increase in data compression with a suitable sparse signal representation before the wireless data transmission at the implant site. Subsequently, we used the correlation-aware two-dimensional DCT used in image processing, to exploit spatial correlation of the data set. In order to guarantee a certain sparsity in the signal representation, two paradigms of zero forcing are evaluated and applied: Significant coefficients- and block sparsity-zero forcing.

Index Terms— Neural Signals, Correlation, Data Compression, Compressed Sensing, Sparse Coding

1. INTRODUCTION

Efficient scale integration and the ongoing decrease of feature size in CMOS processes lead to new fields of microelectronic applications like fully implantable neural measurement systems. These systems can be used for medical diagnostics, neural prostheses or Brain Computer Interfaces (BCIs). The systems are comprised of a multielectrode array (MEA), an analog front-end for signal amplification followed by a signal processing unit and a wireless transceiver. Depending on the application, the number of channels (electrodes) varies from very few electrodes (8-36 for some BCIs [1]) to over 100 electrodes [2] or even more than 1000 [3]. If the electrodes are arranged in close vicinity to each other, a joint processing is possible, otherwise a set of independent measurement systems for each couple of electrodes could be beneficial.

In neural measurement systems the wireless link is often the functional bottleneck in terms of a very limited data rate of a couple of hundred kBit/s [4], or in terms of energy consumption [5], [6]. For the transmission of neural raw data, wireless data rates in the order of 20 MBit/s (100 electrodes

with 10 Bit of resolution and a sample rate of 20 kS/s/channel) could easily occur. In neural measurement system for raw data transmission, complete waveforms instead of extracted signal features are of interest. Especially in medical diagnostics information preservation in neural data could be beneficial (e.g. detection of epileptic disorders).

In order to address the restrictions in terms of bandwidth and/or energy, data compression at the implant site is one possibility of addressing this obstacle. One option to reduce the data rate at the RF transceiver is sparse coding. Sparse coding transforms the signal of interest into a sparse representation with far fewer (significant) signal coefficients compared to the original signal representation. Thus, only the sparse representation of the signal has to be transmitted over the wireless link. At the receiving side, the signal is reconstructed from the sparse representation by an inverse transformation or an appropriate optimization program. Generally speaking, the more structure in the signals is considered by the particular coding scheme, the higher the compression ratio can get. Beside the independent sparse coding of each electrode signal, this work exploits the spatial inter-electrode correlation between adjacent electrodes in order to increase the compression ratio at a given reconstruction accuracy.

Fig. 1 shows a system architecture of an implantable neural measurement system. Neural signals recorded from the multielectrode array will be amplified in the analog front-end (AFE). Subsequently, the neural data runs into the main module where signal processing and data compression take place.
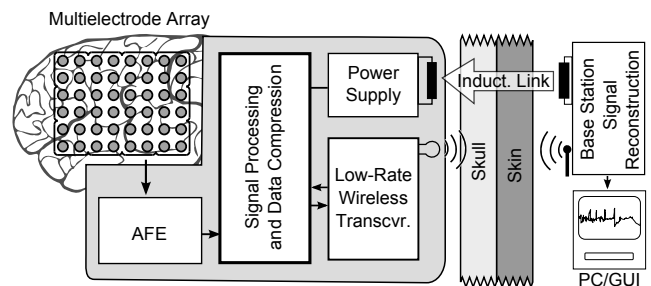
Fig. 1. System architecture of an implantable neural measurement system with a compression unit for neural raw data.
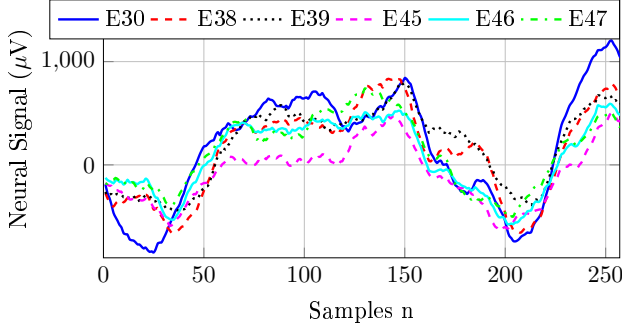
Fig. 2. Example of six correlated neural signals in the time domain, recorded by the surface MEA depicted in Fig.3 for the *a posteriori* known set of electrodes $\{30, 38, 39, 47, 46, 45\}$.

The low-rate wireless transceiver passes the data to the base station, where signal reconstruction is performed. Since the system is fully implantable, energy also has to be transferred wirelessly via an inductive link.

2. SIGNAL CHARACTERISTICS

The neural signals used in this work were recorded invasively from the human brain by the surface MEA depicted in Fig. 3 at the *Epilepsiezentrum Erlangen* (EZE) [7]. This neural signals are sampled at $f_S = 1024$ Hz with a resolution of 16 bits. Therefore, we only consider local field potentials (LFPs) in this work.

Note, in the following we deposit a set of P neural signals with time length N samples in an array $\mathbf{X} \in \mathbb{R}^{P \times N}$. In our first examination of the neural signals provided by the EZE, inter-electrode correlations can be observed, as depicted in Fig. 2 for $P = 6$ correlated neural signals in time domain, recorded by the surface MEA, without prior knowledge of the spatial arrangement of the corresponding electrodes. Subsequent mapping of these correlated neural signals to the surface MEA shown in Fig. 3 revealed a close spatial proximity of the considered electrodes (cmp. Fig. 3, correlated set of electrodes). Therefore, these signal correlations can easily be utilized by a joint compression of locally connected electrodes. This could lead to an improved data compression for certain measurement systems (cmp. Fig.1). Thus, in the following we address $\mathcal{C} = \{30, 38, 39, 47, 46, 45\}$ as a set of correlated and $\mathcal{U} = \{1, 5, 17, 20, 33, 37\}$ as a set of uncorrelated electrodes, respectively neural signals.

2.1. Correlation

In order to measure the similarity between two signals $\mathbf{x}_1 \in \mathbb{R}^N$ and $\mathbf{x}_2 \in \mathbb{R}^N$ we use the *Pearson product-moment correlation coefficient* $r_{x_1 x_2} \in [-1, 1]$ with the following definition

$$r_{x_1 x_2} = \frac{\sum_{i=1}^{N}(x_{1,i} - \bar{x}_1) \cdot (x_{2,i} - \bar{x}_2)}{\sigma_{x_1} \cdot \sigma_{x_2}}, \qquad (1)$$
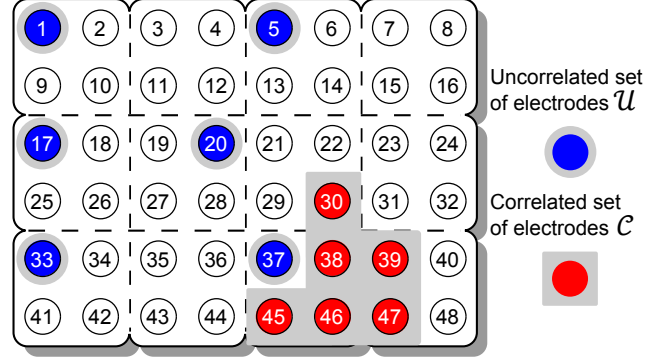
Fig. 3. Schematic electrode layout of the surface MEA (3 mm diameter, 10 mm spacing) with highlighted sets of uncorrelated/correlated electrodes, modified from [9].

Simulation	$\mathbf{r}_{30,38}$	$\mathbf{r}_{38,39}$	$\mathbf{r}_{39,47}$	$\mathbf{r}_{47,46}$	$\mathbf{r}_{46,45}$
signal set $\mathcal{C}$	0.872	0.878	0.852	0.866	0.943
Simulation	$\mathbf{r}_{1,5}$	$\mathbf{r}_{5,17}$	$\mathbf{r}_{17,20}$	$\mathbf{r}_{20,33}$	$\mathbf{r}_{33,37}$
signal set $\mathcal{U}$	-0.028	-0.032	0.019	0.030	-0.018

Table 1. Mean correlation r of a correlated set $\mathcal{C}$ and a uncorrelated set $\mathcal{U}$ of neural signals recorded by a surface MEA.

where $\bar{\mathbf{x}}$ denotes the mean value and σ_x corresponds to the standard deviation of $\mathbf{x}$ [8]. The numerator is called covariance and the denumerator includes statistical spread, which is used for normalization. In case of totally uncorrelated signals the result of Eqn. (1) becomes zero. The following classification is used in order to address the degree of correlation in the neural signals of specific electrodes:

- $0 \leq |r| \leq 0.2$: weak correlation
- $0.2 < |r| \leq 0.5$: medium correlation
- $0.5 < |r| \leq 1$: strong correlation

The categorization of the correlation depends strongly on the utilized signal type. Fig. 2 shows some neural signals from an MEA, which are strongly correlated, according to the mean correlation between two different electrodes listed in Table 1.

Each correlation r between neighboring rows in $\mathbf{X}$ is at least 0.852 in the correlated set $\mathcal{C}$ of neural signals, showing a strong correlation according to the classification. The uncorrelated data set $\mathcal{U}$ exhibits a maximal r of -0.018, thus receiving a weak correlation only.

2.2. Data Compression

Data compression is one of the major tasks in information theory or signal processing [10]. Several techniques can be applied to compress data by identifying and eliminating redundancy or unnecessary information in the signal. This leads to a sparse data representation resulting in K significant coefficients and $(N - K)$ zeros - called sparse coding.

Sparse Coding: Let $\mathbf{x} \in \mathbb{R}^N$ be a (neural) signal in time domain and $\mathbf{c} \in \mathbb{R}^N$ the corresponding K-sparse signal representation due to a basis $\Psi \in \mathbb{R}^{N \times N}$, corresponding to the expression $\mathbf{x} = \Psi\mathbf{c}$. Unfortunately, neural signals are not ideally sparse in a known transform bases [11]. In order to ensure ideal sparsity for the signal representation $\mathbf{c}$, we utilize zero-forcing. Therefore, we applied a threshold for the amplitude- or sample-range in the transform domain, which is called significant coefficients (SC) or block sparsity (BS), respectively, to obtain ideal sparsity by forcing a set of coefficients to zero. By these means we can provide (lossy) data reduction, because for SC we need to only transmit $2K$ values (K for position and K for amplitude) and for BS only K values for the amplitude value in a defined block of samples. These two methods can also be applied for Compressed Sensing to enforce a certain degree of sparsity in the signal of interest. Compressed Sensing is used as a reference compression scheme in this work and is described in the following subsection.

Compressed Sensing: During the last years, new alternatives to traditional data compression techniques were developed, providing resource efficient data compression, inspired by the theory of Compressed Sensing (CS). Therefore, an undersampled signal can successfully be reconstructed with high probability when information about its inherent structure is known a priori [12]. To compress a (neural) signal $\mathbf{x}$ based on CS, $M \ll N$ linear measurements $\mathbf{y} \in \mathbb{R}^M$ are taken, which leads to $\mathbf{y} = \Phi\Psi\mathbf{c}$ described by the basis Ψ and the so-called measurement matrix $\Phi \in \mathbb{R}^{N \times N}$. The vector $\mathbf{c}$ has to be K-sparse to enable CS, whereupon $K < M$. Normally, this constitutes an underdetermined, ill-posed system of equations. But due to the sparsity, signal recovery can be rendered tractably by solving the convex optimization problem

$$\tilde{\mathbf{c}} = \arg \min_{\mathbf{c} \in \mathbb{R}} \|\mathbf{c}\|_1 \quad \text{subject to} \quad \mathbf{y} = \Phi\Psi\mathbf{c}, \qquad (2)$$

as long as $\Phi\Psi$ fulfills the restricted isometry property (RIP) and coherence requirements [13]. Therefore, a sparse signal recovery of all K-sparse signals by l_1-minimization is guaranteed, if at least $M \geq C \cdot K \cdot \log(N)$ measurements are used, where $C > 1$ is a constant. In practice the four-to-one rule $M \geq 4K$ is recommended [14]. Furthermore, in order to enable CS recovery for neural signals, e.g. according to equation (2), a sparsifying basis Ψ has to be chosen.

Discrete Cosine Transform: We applied two forms of a well-known basis, which has adequate compression properties considering neural signals [11].

The discrete cosine transform (DCT) is an extraction of the discrete Fourier transform (DFT) due to mirror symmetry extensions and exploitation of signal symmetries based on cosine functions [15]. Therefore, the DCT is only using real numbers. We used it in order to transform the signal $\mathbf{x} \in \mathbb{R}^N$ to frequency domain, which has adequate compression prop-

erties due to signal decorrelation [16]. That implies a process which reduces auto-correlation within a signal or cross-correlation within a set of signals, while preserving other aspects of the signal. In general the DCT^{II} definition,

$$\mathbf{c}_n = \sum_{b=0}^{N-1} \mathbf{x}_b \cdot \cos\left(\frac{\pi}{N}(b + 1/2)n\right), \qquad (3)$$

is used for data compression, which implies the boundary conditions of the signals. Hence, $\mathbf{c}_n$ as a function of n is *even* around $n = 0$ and *even* around $n = N$.

Two-Dimensional Discrete Cosine Transform: In order to compress a set of signals we can transform each signal by using a one-dimensional DCT or applying a two-dimensional discrete cosine transform (DCT2) is a straightforward extension of the DCT^{II}

$$\mathbf{C}_{p,n} = \sum_{a=0}^{P-1} \sum_{b=0}^{N-1} \mathbf{X}_{a,b} \cdot \cos\left(\frac{\pi}{N}(b + 1/2)n\right)$$
$$\cdot \cos\left(\frac{\pi}{P}(a + 1/2)p\right). \qquad (4)$$

A DCT2 analyzes a set of signals in terms of time and spatial variations and the linear combination of both variations. This results in a two-dimensional representation, which could including only a few large coefficients depending on frequencies within the signals. Therefore, in contrast to DCT, only DCT2 is able to consider a spatial correlation in a (neural) set of signals.

Figure of Merit: In order to address the degree of sparsity for the signal representation $\mathbf{c}$ by a certain transform basis Ψ, we use the quotient $\text{CR} = N/K$, which denotes the achievable compression ratio $\text{CR} \in \mathbb{R}$. The sparser the representation of the signal, the higher the achievable compression ratio.

A criterion to measure the quality of the reconstructed signal $\hat{\mathbf{x}}$, compared to the original signal $\mathbf{x}$, is the signal-to-noise-and-distortion ratio (SNDR),

$$\text{SNDR} = 10\,\text{dB} \cdot \log\left(\frac{\|\mathbf{x}\|_2^2}{\|\mathbf{x} - \hat{\mathbf{x}}\|_2^2}\right), \qquad (5)$$

as another figure of merit (FOM) [17]. The argument of the logarithm is equivalent to the inverse of the so-called normalized Mean Squared Error (MSE).

3. RESULTS AND DISCUSSION

In this section we exploit correlation in neural signals to obtain a gain of data compression using sparse coding. Therefore, we consider two sets of neural signals with a length of $N = 256$ samples, which are recorded by a surface MEA. By selecting certain electrodes in the array $\mathbf{X}$, we get a correlated set $\mathcal{C}$ and uncorrelated set $\mathcal{U}$ of neural signals, as referred in
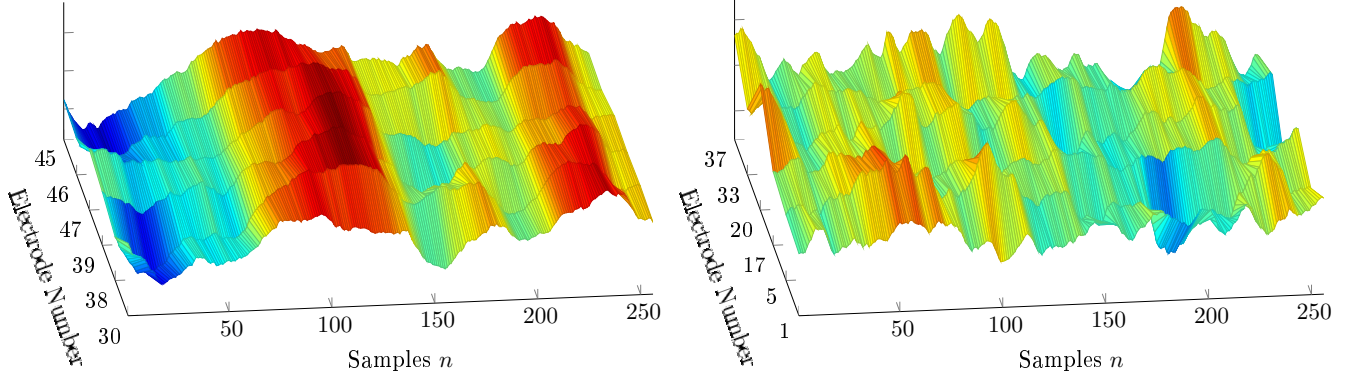
Fig. 4. One sequence of 256 Samples of correlated electrode set $\mathcal{C}$ (left handside) and uncorrelated electrode set $\mathcal{U}$ (right handside) neural signals recorded by a surface MEA (cmp. Fig. 3). The intensity of the color denotes the amplitude value in μV. For the electrodes $\mathcal{C}$ a high inter-electrode correlation with smooth transitions is observed. In contrast to this, the electrodes $\mathcal{U}$ exihbit high frequency contents.

Simulation	$\mathrm{CR_{SC}}$	$\mathrm{CR_{BS}}$	$\mathrm{CR_{CS}}$
DCT on signal set $\mathcal{U}$	4.18	5.33	1.73
DCT2 on signal set $\mathcal{U}$	3.91	5.33	
DCT on signal set $\mathcal{C}$	9.11	9.85	3.05
DCT2 on signal set $\mathcal{C}$	10.12	9.85	

Table 2. Mean CR for a mean SNDR ≈ 11 dB for SC-/BS-zero forcing and CS using DCT and DCT2 of uncorrelated set $\mathcal{U}$ (top) and correlated set $\mathcal{C}$ (bottom) of neural signals ($N = 256$) recorded by a surface MEA (cmp. Fig. 3).

section 2.1 and depicted in Fig. 3, which are subject to the following investigations. Furthermore, we itemize CS as a reference compression scheme for our results.

Fig. 4 shows the amplitudes of six correlated and uncorrelated neural signals. It can be seen that the set of correlated signals exhibits a high vertical structure visible in form of electrode independent vertical bars. We took advantage of the spatial correlation between each neural signal pair (rows in **X**), which reflects an image-related structure. Due to the vertical structure less high frequency coefficients are needed in the transform domain, because of the smooth signal progression. Therefore, the usage of a two-dimensional transform on correlated (neural) data is advantageous and is expected to lead to higher compression ratios.

In order to evaluate the two sets of neural signals in terms of compression properties, we consider the CR and SNDR as figures of merit, as introduced in section 2.2. Furthermore, we apply SC- and BS-zero forcing to ensure an ideally sparse signal representation by using DCT or DCT2 for correlated and uncorrelated signals, respectively. The results in CR at a certain SNDR for DCT/DCT2 are compared to those of CS (considering SC-zero forcing for ideal sparse signal representation), acting as a reference compression scheme. The increasing of CR causes a decreasing of SNDR, depending on

the used signal and basis [11]. For the CS simulations, CVX was used to solve the l_1-minimization problem [18].

The upper part of Table 2 shows the mean compression ratios (CR) for a given SNDR of approximately 11 dB applied to the set of uncorrelated neural signals. The difference in CR with SC-zero forcing is a consequence of the additional high vertical frequency components of the signal set $\mathcal{U}$ in the DCT2 domain compared to the DCT, leading to a higher amount of frequency coefficients above threshold, thus decreasing the CR. Due to the threshold for small frequency coefficients, SC obtains much more sparsity than BS, however for SC the positions of the frequency coefficients have to be transmitted too, ending up in a CR divided by two, as shown in Table 2. Furthermore, the $\mathrm{CR_{BS}}$ remains constant due to the identical block-size for BS-zero forcing applied on DCT and DCT2. Compared to SC, we observe an increased CR of BS-zero forcing for both transform schemes by this correlation-independent block-size implementation.

In the lower part of Table 2 the figure of merit for correlated neural signals, recorded from neighboring electrodes (cmp. Fig. 3) is shown. Again, in order to evaluate the achievable CR we targeted approximately the same SNDR of 11 dB for a better comparability. Due to the smooth spatial (vertical) structure of the correlated signals (cmp. Fig. 4) the DCT2 signal representation needs less large frequency coefficients, which results in a higher CR, compared to the DCT for SC-zero forcing of correlated signals in set $\mathcal{C}$. Furthermore, in contrast to the upper part of Table 2 DCT2 on correlated (neural) signals achieve an increased CR for SC-forcing compared to BS. In contrast to CS, both zero forcing methods exihbit highter CRs independent of the degree of correlations in $\mathcal{U}$ and $\mathcal{C}$.

The comparison of compression properties between correlated and uncorrelated neural signals performing DCT and DCT2 with SC-zero forcing is illustrated in Table 3. For the enforced sparsity of the signal representation we used similar

Simulation	signal set $\mathcal{U}$	signal set $\mathcal{C}$
$\Delta \mathbf{CR_{SC,(DCT2-DCT)}}$	-0.27	+1.01

Table 3. Gain of $\mathbf{CR_{SC}}$ based on Table 2, when using DCT2 instead of DCT for the signal sets $\mathcal{U}$ and $\mathcal{C}$, respectively.

signal qualities (SNDR $\approx 11\,\text{dB}$) in both cases. According to Table 3 a relative gain in CR of $+1.01$ for correlated signals is achievable. As a consequence exploiting correlated (neural) signals for adequate joint data compression using a two-dimensional transform bases like DCT2 is recommended.

4. CONCLUSION

This paper deals with the spatial correlation in neural signals and evaluates different compression schemes to make use of this signal feature in sensor systems where the data rate of the wireless link is the most severe constraint. The exploitation of correlation by grouping neighboring electrodes leads to a significant improvement in data compression with a proper kind of sparse signal representation using DCT2 for sparse coding. Therefore, in order to guarantee a certain sparsity in the signal representation, the paradigms of significant coefficients- and block sparsity-zero forcing are evaluated and applied. Also Compressed Sensing was evaluated as a possible compression scheme, trading lower CRs (cmp. Table 2) for a reduced hardware complexity at the transmitter, which could be beneficial especially for neural measurement systems with a high channel count (more than 22 channels [19]). As stated above, real measurements of neural signals were available for our examination. We showed a significant increase in terms of compression ratio (CR) at a given SNDR for correlated neural signals using DCT2 compared to uncorrelated data.

REFERENCES

[1] W.-K. Tam, K. Tong, F. Meng, and S. Gao, "A minimal set of electrodes for motor imagery BCI to control an assistive device in chronic stroke subjects: A multi-session study," *IEEE Transactions on Neural Systems and Rehabilitation Engineering*, 2011.

[2] J. Pistor, J. Hoeffmann, D. Rotermund, and E. Tolstosheeva et al., "Development of a fully implantable recording system for ECoG signals," in *Design, Automation & Test in Europe Conference & Exhibition (DATE)*, 2013.

[3] K. D. Wise, D. J. Anderson, J. F. Hetke, D. R. Kipke, and K. Najafi, "Wireless implantable microsystems: high-density electronic interfaces to the nervous system," *Proceedings of the IEEE*, vol. 92, Jan. 2004.

[4] Zarlink Semiconductor (now: Microsemi), "ZL70102-Medical implantable RF transceiver MICS RF telemetry," June 2010.

[5] F. Chen, A. P. Chandrakasan, and V. M. Stojanovic, "Design and analysis of a hardware-efficient compressed sensing architecture for data compression in wireless sensors," *IEEE Journal of Solid-State Circuits*, vol. 47, no. 3, pp. 744 –756, Mar. 2012.

[6] F. Chen, F. Lim, O. Abari, A. Chandrakasan, and V. Stojanovic, "Energy-aware design of compressed sensing systems for wireless sensors under performance and reliability constraints," *Circuits and Systems I: Regular Papers, IEEE Transactions on*, 2013.

[7] Epilepsiezentrum Erlangen (EZE), "Daten der neurologischen Klinik - Epilepsiezentrum," 2013.

[8] L. Fahrmeir, R. Künstler, I. Pigeot, and G. Tutz, *Statistik: Der Weg zur Datenanalyse*, 2007.

[9] AD-TECH Medical Instrument Corporation, "Subdural Electrodes REF: FG48G-SP10X-0CB," 2013.

[10] D. Salomon, *A Concise Introduction to Data Compression*, Undergraduate Topics in Computer Science. London, 2008.

[11] S. Schmale, B. Knoop, J. Hoeffmann, D. Peters-Drolshagen, and S. Paul, "Joint compression of neural action potentials and local field potentials," *47th Asilomar Conference on Signals, Systems and Computers*, Nov. 2013.

[12] Y. C. Eldar and G. Kutyniok, *Compressed Sensing Theory and Applications*, Cambridge University Press, 2012.

[13] E. J. Candès, "The restricted isometry property and its implications for compressed sensing," *Comptes Rendus Mathematique*, vol. 346, pp. 589–592, 2008.

[14] E. J. Candès and M. B. Wakin, "An introduction to compressive sampling," *Signal Processing Magazine, IEEE*, vol. 25, no. 2, pp. 21–30, March 2008.

[15] K. R. Rao and P. Yip, *Discrete Cosine Transform-Algorithms, Advantage and Applications*, Academic Press Limited, 1989.

[16] T. Strutz, *Bilddatenkompression: Grundlagen, Codierung, Wavelets, JPEG, MPEG, H.264*, 2009.

[17] F. Chen, A. P. Chandrakasan, and V. Stojanovic, "A signal-agnostic compressed sensing acquisition system for wireless and implantable sensors," in *2010 IEEE Custom Integrated Circuits Conference (CICC)*, 2010.

[18] CVX Research Inc., "Cvx: Matlab software for disciplined convex programming, version 2.0 beta," 2012.

[19] A. M. Abdulghani, A. J. Casson, and E. Rodriguez-Villegas, "Quantifying the feasibility of compressive sensing in portable electroencephalography systems," in *Foundations of Augmented Cognition. Neuroergonomics and Operational Neuroscience*. 2009.